Hidden Fermi liquid; the moral: a good effective low-energy theory is worth all of Monte Carlo with Las Vegas thrown in

2010 J. Phys.: Condens. Matter 22 164201

(http://iopscience.iop.org/0953-8984/22/16/164201)

J. Phys.: Condens. Matter **22** (2010) 164201 (5pp) doi:10.1088/0953-8984/22/16/164201

Hidden Fermi liquid; the moral: a good effective low-energy theory is worth all of Monte Carlo with Las Vegas thrown in

Philip W Anderson and Philip A Casey

Department of Physics, Princeton University, Princeton, NJ 08544, USA

E-mail: pwa@princeton.edu

Received 3 October 2009, in final form 11 January 2010
Published 30 March 2010
Online at stacks.iop.org/JPhysCM/22/164201

Abstract

We present a formalism for dealing directly with the effects of the Gutzwiller projection implicit in the t–J model which is widely believed to underlie the phenomenology of the high-T_c cuprates. We suggest that a true Bardeen–Cooper–Schrieffer condensation from a Fermi liquid state takes place, but in the unphysical space prior to projection. At low doping, however, instead of a hidden Fermi liquid one gets a 'hidden' non-superconducting resonating valence bond state which develops hole pockets upon doping. The theory which results upon projection does not follow conventional rules of diagram theory and in fact in the normal state is a $Z = 0$ non-Fermi liquid. Anomalous properties of the 'strange metal' normal state are predicted and compared against experimental findings.

(Some figures in this article are in colour only in the electronic version)

1. Introduction

The following is taken from the lecture as given and is a discursive summary of a several year program. Readers who may want more detail are urged to look at the more extensive calculations and experimental comparisons in [1–4] and other papers on arXiv. We would note that many of the data for which agreement is claimed (the tunneling asymmetry and shape, shapes of EDCs (energy distribution curves) in ARPES, power law behavior of $\sigma(\omega)$, normal state resistivity) are of a detailed nature which alternative theories do not attempt to explain or compute.

The story starts with a question we first encountered five years ago from Doug Scalapino: 'Why is it that the electrons in the cuprates can be described by quasiparticles in the superconductor, but in the normal state do not look at all like a Fermi liquid?' The answer: because there *is* a Fermi liquid in the problem, undergoing a BCS transition. But it's *hidden* because its quasiparticles are not the real physical electrons. In the 'normal' state, the strange metal, the wavefunction renormalization connecting the two, Z, is zero. When the gap opens, Z becomes finite; there is a coherent quasiparticle.

The solution to this paradox: Gutzwiller projection. This is not a mathematical trick, it's a physical fact. Doing cuprates without Gutzwiller projection is abandoning the attempt to find a low-energy effective theory, since it leaves us with matrix elements connecting to high-energy doubly occupied states.

It is therefore fundamental to transform to a projected Hamiltonian,

$$H_{t-J} = \mathrm{e}^{\mathrm{i}S} H_0 \mathrm{e}^{-\mathrm{i}S} = PtP + J\sum_{i,j} S_i \cdot S_j$$
$$P = \prod_i (1 - n_{i,\uparrow} n_{i,\downarrow}). \tag{1}$$

Eigenstates (ground and single-particle excitations) *must* be of the form,

$$\Psi = P\Phi(r_1, r_2, \ldots, r_N) \tag{2}$$

so we try to find Φ variationally. We make the obvious Hartree–Fock–BCS ansatz:

$$\Phi = \prod_k (u_k + v_k c^*_{k\uparrow} c^*_{-k\downarrow})\Psi_{\mathrm{vac}} \tag{3}$$

and determine the coefficients u_k and v_k variationally, thus acquiring a set of gap equations.

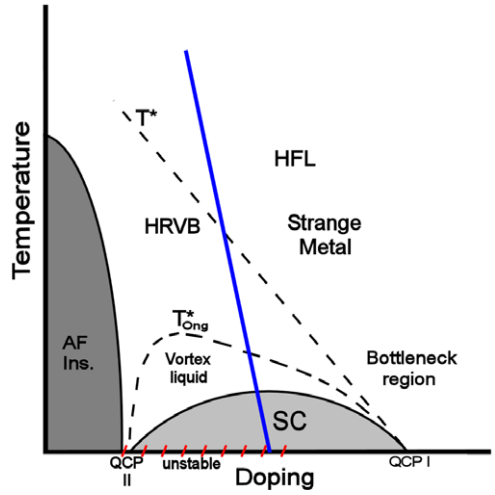

Figure 1. Revised cuprate phase diagram including the HFL and HRVB regions (the crossover between the two regions is shown by the blue line).

2. Gutzwiller projected Fermi sea: the 'hidden' FL

Ansatz: the *unprojected* low-energy states of a strongly correlated (that is, with an upper Hubbard band) Fermi gas can be chosen to be a Fermi liquid (if no gap). That is, in equations:

$$P = \prod_i (1 - n_{i,\uparrow} n_{i,\downarrow}) \qquad T = \sum_{i,j,\sigma} t_{ij} c^*_{i\sigma} c_{j\sigma}$$
$$H = \mathrm{PTP} \qquad \Psi = P\Phi \tag{4}$$

$H\Psi = E\Psi$ is the same as $H\Phi = E\Phi$. Φ *not* Ψ, is assumed to have Fermi liquid properties: the hidden Fermi liquid [5].

2.1. Another possibility: the hidden RVB (HRVB)

Suppose $J \gg$ PTP. J will control the 'hidden' structure, an RVB, not a Fermi liquid. The 'Fermi surface' is four point nodes which expand into Rice–Zhang 'pockets' of Fermi surface upon doping. Yang *et al* [6] have made a good start at this theory, all indications suggest it is right (see [7] for example) for well underdoped cases. These cases are not competitors but rather two different limits! The crossover is challenging. Keep tuned as much is happening, but that is not this talk. Our proposed new phase diagram has a crossover line separating the HFL from the HRVB regimes (figure 1).

Returning to the HFL, if Φ_0 is the ground state of this problem, $c_{k\sigma}\Phi_0$ for $k < k_\mathrm{F}$ and $c^*_{k\sigma}\Phi_0$ for $k > k_\mathrm{F}$ create eigen-excitations with finite amplitude Z, if k is near a sharp Fermi surface, determined by Hartree–Fock equations using projected H. Why?—Why not? Shankar's 'poor man's renormalization' [8] seems to apply—all Fermi systems renormalize to FL in shell around FS (figure 2). They also create pieces in the upper Hubbard band, but these are projected away by the Hamiltonian and don't mix (figure 3). Since these two problems are equivalent, $P = P^2$, these are also excitations of the *real* problem. But we cannot access them directly via real one-particle operators because $Pc \neq cP$. The

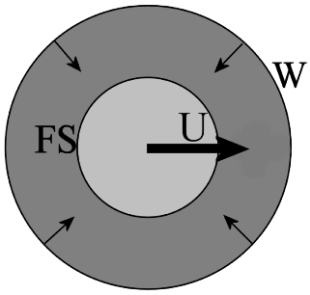

Figure 2. Schematic of the starting point for the 'poor man's renormalization' technique. The cutoff, W, is chosen to be beyond the largest energy scale of the problem, U. Subsequently, the excess phase space is squeezed down to a small shell, encompassing U, about the Fermi surface.

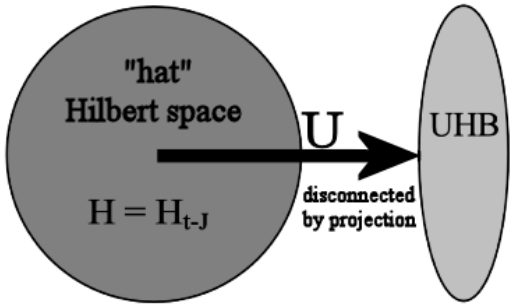

Figure 3. Illustration of when the low-energy spectrum terminates at an energy lower than the largest energy scale of the problem, U. One then projects away these high-energy states (the upper Hubbard band) and uses the remaining states, which do not mix with the UHB, to calculate observables.

real one-particle operators are,

$$\hat{c_{i\uparrow}} = c_{i\uparrow}(1 - n_{i\downarrow} n_{i\uparrow}) = c_{i\uparrow} c_{i\downarrow} c^*_{i\downarrow} = \sum_{k,k',k''} c_{k\uparrow} c_{k'\downarrow} c^*_{k''\downarrow} \tag{5}$$

and similarly for $c^* P = \hat{c^*}$. These operators will automatically keep us within the lower Hubbard band, so 'all' we need to do is to evaluate the Green's function of a three-Fermion operator.

This looks like a hopeless mess but it isn't. Because of the strong exclusion principle restrictions on momentum, and to make the creation of real pseudoparticles energetically possible, all have to be near the Fermi surface and traveling in the same direction. Two factorizations are important:

$$\hat{c_{k\uparrow}} \approx \sum_q (c_{k-q\uparrow} \rho_{q\downarrow} + c_{k-q\downarrow} S^+_q) \tag{6}$$

ρ and S^+ are density and spin Tomonaga waves moving in the direction of the Fermi velocity $v_\mathrm{F}(k)$. Haldane has shown that these bosons are a valid alternative representation of a Fermi liquid [9].

2.2. Green's function of the HFL

To get spectra we have to calculate Green's functions of the 'hat' operators. For tunneling,

$$G(i,t) = \langle \hat{c^*_{i\sigma}}(t) \hat{c_{i\sigma}}(0) \rangle \tag{7}$$

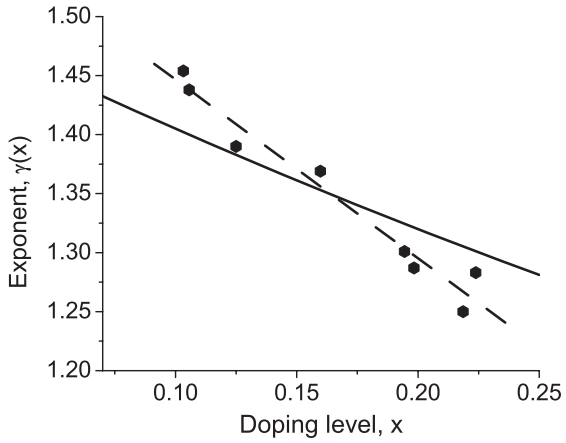

Figure 4. Infrared spectrum exponents for $Bi_2Sr_2CaCu_2O_{8+\delta}$. Data points from [11] with linear best fit of [11] (dashed line) and predicted value from [2] (solid line). The predicted exponent stems from $\sigma(\omega) = (i\omega)^{-2+\gamma}$ with $\gamma = 1 + 2p$, and p is given in the text. Figure reproduced with permission from [3]. Copyright 2008 by Macmillan Publishers Ltd.

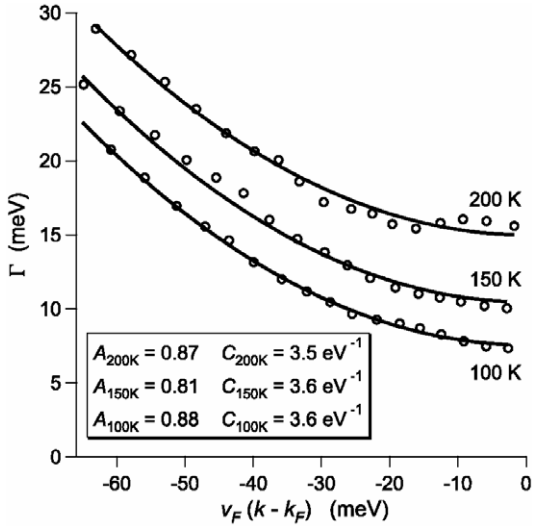

Figure 5. Relaxation rate, Γ, (data points) extracted by fitting the experimental EDCs. The 'Doniach–Sunjic' functional form for the EDCs was derived in [3]. The solid lines are best fits to $\Gamma = Ak_BT + Cv_F^2(k - k_F)^2$. The given empirical values fit well to universal parameters $A = 0.85$ and $C = 3.6\ \mathrm{eV}^{-1}$.

and for ARPES,

$$G([r_i - r_j], t) = \langle \hat{c}_\sigma^*(r_i, t)\hat{c}_\sigma(r_j, 0)\rangle \tag{8}$$

plus the irrelevant part that goes into the upper Hubbard band.

The averages denoted by $\langle\,\rangle$ are ground state at $T = 0$, or thermal at finite T. These are surprisingly easy because they factorize, using equations (6) and Fermi liquid rules (spins independent of each other), into $G_{\mathrm{free}}G^*(t)$.

The effect on the tunneling spectra was evaluated in [2]. At absolute zero, $G^*(t)$ is the x-ray line problem of Doniach–Sunjic and is t^{-p} with $p = 2(1 - x)^2/8$ (the factor of 2 for the two channels in equation (6)). The final result is a power law Fermi surface singularity:

$$\frac{\mathrm{d}I}{\mathrm{d}V} \propto \omega^p \tag{9}$$

and at finite T,

$$\frac{\mathrm{d}I}{\mathrm{d}V} \propto \mathrm{Re}\{(AT - i\omega)^p\}. \tag{10}$$

Where does the power law come from? Friedel's theorem, basically: in order to change the number of electrons locally, you have to shift the phase of the whole electron gas and, eventually, push electrons out through the boundary. Via the 'orthogonality catastrophe' this causes power law corrections to wavefunction overlaps [2].

To get EDCs (i.e. Green's functions) we rely on Huygens' principle. That is, $G^*(t)$ is common to all, so Green's function in r, t space is $G_0(r - v_Ft)G^*(t)$. To calculate the IR conductivity we use the simple bubble diagram with no vertex correction, and take $\omega \gg T$ (both valid approximations). Since early work of Schlesinger and Collins [10] it has been known that σ is a power law:

$$\sigma(\omega) \propto (i\omega)^{-1+2p}. \tag{11}$$

There have been many measurements since 1989, the latest being from Timusk (see figure 4) [11].

2.3. Finite temperature—a kluge

At finite T, Yuval observed that the integral becomes periodic in imaginary time with period $2\pi T$ [12].

$$t^{-p} \to [\sinh(\pi Tt)/\pi T]^{-p}. \tag{12}$$

This we approximate as,

$$G^*(t) \propto t^{-p}e^{-\Gamma t}. \tag{13}$$

Here we take $\Gamma = Ak_BT + Cv_F^2(k - k_F)^2$, A is close to unity ($p\pi$ is a guess) but C is the only arbitrary fitting parameter—a way of adding in the umklapp scattering rate in the HFL.

It is now easy to Fourier transform to get a 'Doniach–Sunjic' lineshape for the EDCs. Fitting to Dessau and Koralek's experiments [13], Casey could get the parameter values in figure 5 [3]. The $(k - k_F)^2$ dependence came from this fit, and was a pleasant surprise. We have used C to estimate the T^2 relaxation of the HFL: it agrees well with the $1/T^2$ Hall effect relaxation time (a long-standing puzzle) [4].

3. Superconducting state

The reason for the power law decay of $G^*(t)$ is the infrared catastrophe. But with a gap, IR catastrophe goes away. To calculate lineshapes, we need to do the Doniach–Sunjic in a superconductor. Fortunately, there is a crib: Ma [14]. Casey has calculate a typical EDC, as seen in figure 6. Near optimal doping, therefore, it is fairly accurate to calculate using only the coherent spectrum [1] and get a good simulacrum of tunneling spectrum *complete with universal asymmetry*! Without projection cannot explain asymmetry in point contact tunneling (Wannier's theorem).

Dessau's typical results [13] are more like our prediction than previous attempts, but still not very good. (i) In the

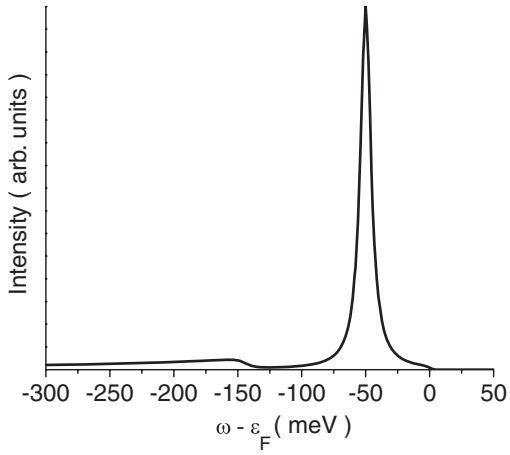

Figure 6. Representative EDC based on Ma's calculation of the 'Doniach–Sunjic' lineshape in a superconductor [14] at $T = 20$ K, $\Delta = 50$ meV, and $\Gamma = 5$ meV.

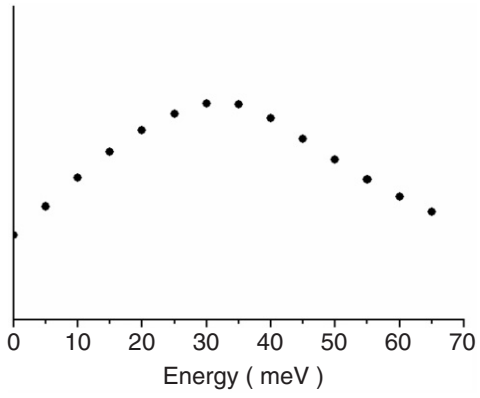

Figure 7. 'Hump' in tunneling spectrum, $\int \chi''(\omega) D(E)\, \mathrm{d}E$, estimated from Hinkov's susceptibility data [17] and Pan's tunneling data [18][1] . The energy is measured from the coherence peak which should be imagined to be added in around $E = 0$ with a total area comparable to that of the hump.

real data, the peaks are ragged rather than broadened—this must be gap inhomogeneity, as emphasized by Yazdani [15]. (ii) There's much too big a background, at too low energy. What is new?

D-wave superconductivity greatly enhances the spin susceptibility and lowers the energy of spin fluctuations in the general region of (π, π) (because of coherence factors). The system is starting to see AF instability (note that AF and d-wave help each other, not compete). Again, the trick is to factorize the 'hat' operator and hence Green's function,

$$c_{i\sigma} = c_{i\sigma} c_{i-\sigma} c^*_{i-\sigma} = c_{i-\sigma} S^-_i \tag{14}$$

or

$$c_{i\sigma} = c_{i\sigma}(1 - n_{i-\sigma}) \tag{15}$$

$$G(0,t) = \langle 0|\hat{c^*_{i,\uparrow}}(t) c_{i,\uparrow}(0)|0\rangle = G_{\text{coherent}} + G_{\text{inc,density}} + G_0(0,t)\langle 0|S^+_i(t) S^-_i(0)|0\rangle. \tag{16}$$

The last term is the contribution from the resonance. Since G_0 is sharply peaked in energy, the shape of the background is that of the susceptibility (work of Phil Casey), as seen in figure 7, and the hump in optimally doped BiSCCO [16].

$$\int \mathrm{d}t\, \mathrm{e}^{\mathrm{i}\omega t} \langle 0|S^+_i(t) S^-_i(0)|0\rangle = \chi''_i(\omega) = N^{-1} \sum_k \chi''(k,\omega). \tag{17}$$

ARPES is a much harder problem—but clearly, as observed, there will be a big increase in background for states which can scatter at (π, π). But, crossover to HRVB?

3.1. Resistivity in the strange metal: the bottleneck effect

There are two *different* dissipative processes for accelerated electrons. One may be thought of as the decay of quasiparticles—which are what the electric field sees—into pseudoparticles, which are the true excitation spectrum. The second is the scattering rate of the pseudoparticles, which is a simple Fermi liquid with T^2 dependence. These two processes act in series to dissipate the momentum to the lattice. This

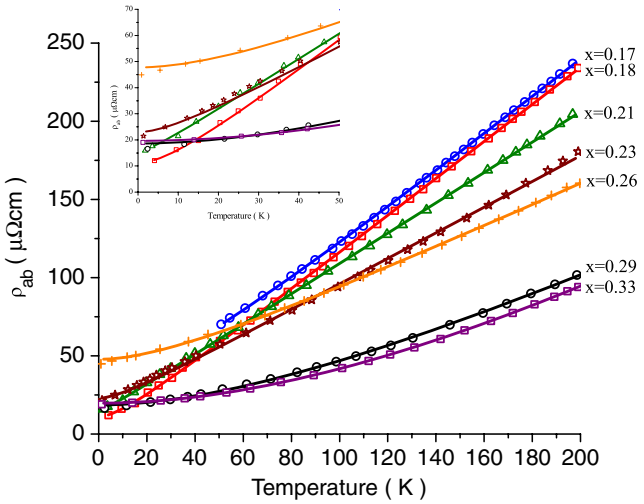

Figure 8. Comparison of $La_{2-x}Sr_xCuO_4$ resistivity (data points) extracted from [19] with the bottleneck resistivity form of equation (18). Details of the fits and functional parameters can be found in [4]. The inset shows low temperature region in detail.

means that the slowest one controls the rate of dissipation, not the fastest. That is, it's an anti-Matthiessen rule: the conductivities add, not the resistivities! This is the *bottleneck effect* [4].

$$\rho \propto (1/T + T_0/T^2)^{-1} = T^2/(T + T_0). \tag{18}$$

This magic formula fits a lot of early data like a glove, as can be seen in figure 8. Note that it is T^2 at low T, linear with negative intercept at high—puzzling characteristics from the beginning.

4. Remarks and conclusion

Conventional perturbation theory won't work: analytic structure is cuts, not poles. When we go superconducting

[1] We are indebted to S H Pan for extracting the curve we show from the extensive data on which the paper is based.

gapping of Tomonagons allows real quasiparticles—but the tail is still not integrable! Manipulations of conventional diagram theory a la Eliashberg theory [20, 21] are not legitimate because the conditions for its validity are not satisfied. They lead to misinterpretations of simulational or experimental data. (For instance, hole-particle asymmetry does not occur within Eliashberg though it is manifest in the data.) It appears we now have a systematic controlled formalism for Gutzwiller projection which works and is useful—please give it a try! A similar formalism may work for HRVB. It also appears laser ARPES is fantastically accurate (recent data from Zhou in China confirms Dessau). The bottleneck effect seems rather ubiquitous—we find heavy-electron and organic systems with the characteristic resistivity shape and the 'linear T' resistivity often ascribed to QCPs is probably this instead, most of the time. Casey is systematically going through other transport phenomena—Kadowaki–Woods, Wiedemann–Franz—and getting agreement.

References

[1] Anderson P W and Ong N P 2006 *J. Phys. Chem. Solids* **67** 1–5
[2] Anderson P W 2006 *Nat. Phys.* **2** 626–30
[3] Casey P A *et al* 2008 *Nat. Phys.* **4** 210–2
[4] Anderson P W and Casey P A 2009 *Phys. Rev.* B **80** 094508
[5] Anderson P W 2008 *Phys. Rev.* B **78** 174505
[6] Yang K Y, Rice T M and Zhang F C 2006 *Phys. Rev.* B **73** 174501
[7] Meng J *et al* 2009 *Nature* **462** 335–8
[8] Shankar R 1994 *Rev. Mod. Phys.* **66** 129–92
[9] Haldane F D M 1994 *Varenna Lectures 1992* ed R A Broglia and J R Schrieffer (Amsterdam: North-Holland)
[10] Schlesinger Z *et al* 1990 *Phys. Rev. Lett.* **65** 801
[11] Hwang J, Timusk T and Gu G D 2007 *J. Phys.: Condens. Matter* **19** 125208
[12] Yuval G and Anderson P W 1970 *Phys. Rev.* B **1** 1522–8
[13] Koralek J D *et al* 2006 *Phys. Rev. Lett.* **96** 017005
[14] Ma Y 1985 *Phys. Rev.* B **32** 1472–5
[15] Gomes K K *et al* 2007 *Nature* **447** 569–72
[16] Anderson P W and Casey P A 2009 arXiv:0902.1980v1
[17] Hinkov V *et al* 2007 *Nat. Phys.* **3** 780
[18] Hudson E W *et al* 1999 *Science* **285** 88
[19] Cooper R A *et al* 2009 *Science* **323** 603
[20] Hwang J, Timusk T, Schachinger E and Carbotte J P 2007 *Phys. Rev.* B **75** 144508
[21] Maier T A, Poilblanc D and Scalapino D J 2008 *Phys. Rev. Lett.* **100** 237001